13 Basal Cell Carcinoma Ultrasound Examination with 20 and 75 MHz High-Frequency Ultrasound

Artur Bezugly

Abbreviations

BCC	Basal cell carcinoma
HFUS	High-frequency ultrasound
ICC	Intraclass correlation coefficient
SCC	Squamous cell carcinoma

Introduction

Malignant skin tumors are the most common among all malignant neoplasms [1–3].

The stage of the tumor process directly affects the treatment result. Therefore, in the modern scientific literature, an early, timely, and late diagnosis level is distinguished [4, 5].

It is essential to achieve the diagnosis in the early tumor development stages—in situ or stages T1, N0, and M0. At this early stage, correctly selected therapy can guarantee a very high probability of complete recovery [6, 7].

Many skin lesions are determined by visual examination. However, the need for differential diagnosis entails specific difficulties for primary care specialists as well as oncologists and dermatologists [4, 7].

The primary diagnostic technique for skin tumors is a visual examination of the lesion on the skin. The visual assessment's main task is to study and characterize a skin tumor's appearance and identify its morphological elements. The topical component is also considered since some skin neoplasms have a favorite localization (for example, basal cell carcinoma in the face) [1, 2, 7].

The visual assessment of skin neoplasms can be improved using dermoscopy and videodermoscopy. According to current data, dermoscopy significantly increases the diagnosis's accuracy and specificity, confirmed by histological examination results [8]. High-frequency ultrasound (HFUS) is used for internal skin structure assessment in both normal and pathological conditions, which improves the diagnostic possibilities of dermatologists and oncologists. The high-frequency examination allows accurate and fast discrimination of epidermal, dermal, and subcutaneous tissues in real time. This procedure helps identify lesions that are not visible to the human eye. High resolution is used to accurately visualize and measure skin lesions [9, 10]. Tumor boundaries and invasion depth preoperative determination are essential for treatment effectiveness increasing and recurrence risk reduction [2, 10].

The high-frequency ultrasound in the range of 20–75 MHz has enough resolution of 80–21 μm,

A. Bezugly (✉)
Department of Dermatology and Cosmetology, Institution- Academy of Postgraduate Education under the Federal State Budgetary Unit Federal Scientific and Clinical Center for Specialized Medical Assistance and Medical Technologies of the Federal Medical Biological Agency, Moscow, Russia

X. Wortsman (ed.), *Textbook of Dermatologic Ultrasound*,
https://doi.org/10.1007/978-3-031-08736-3_13

and high-frequency skin images are closer to histology. A comparison of the skin tumor's ultrasonographic and histological depth measurements provided in many studies has shown good correlations.

There is no exact matching of high-frequency and histological measurements because high-frequency assessment is provided in vivo, and histological examination is carried out on tissues that have been treated with formalin and dyes.

Moreover, there are no blood vessel filling and hydrostatic blood pressure in the histological specimen. Due to fixation with formaldehyde and dye impregnation, the tissue volume decreases. Thus, the histologic measurement results are usually slightly less than those obtained using high-frequency ultrasound in vivo.

Literature Review

In 1987, Schwaighofer et al. provided 26 malignant melanoma HFUS evaluations and reported a high correlation between the sonographically measured maximal tumor thickness values and those determined postoperatively in histology [11].

Hoffmann et al. (1989) provided skin tumor HFUS thickness and margin assessment on 236 patients. The HFUS accuracy in melanoma thickness and BCC invasion depth determination was obtained [12].

In 1990, Hoffmann et al. described BCC HFUS features at a 20 MHz frequency. BCC was described as a well-defined area with poor echoes, sometimes anechoic [13]. The authors described the tumor structure inhomogeneity and post-tumoral signal reflection enhancement and noted an exact correlation between BCC histological and sonographic images.

Gassenmaier et al. (1990) obtained a strong correlation (r = 0.97) between preoperative 20 MHz HFUS and postoperative histologic tumor thickness determination in 72 primary malignant melanomas [14].

Bahmer et al. (1990) measured vertical tumor thickness with HFUS in 30 benign and malignant skin tumors of various shapes and showed a correlation coefficient of r = 0.77 between tumor volume and its maximal vertical thickness [15].

Harland et al. (1993) reported about a strong correlation between histology and ultrasound for maximal tumor depth measurements (r = 0.96, $p < 0.0001$), and less good for maximal width (r = 0.84, $p < 0.0001$), most probably because of the elastic contraction of tissue at excision [16].

Gupta et al. (1996) obtained the significant correlation between the BCC depth measured histologically and 40 MHz HFUS (p = 0.0004, r = 0.92) [17].

Krähn et al. (1997) studied melanocytic skin lesions at 20 MHz and determined tumor thickness before surgery. High correlation between HFUS and histologic results was obtained for nevi (r = 0.93) and melanoma (r = 0.95) [18].

Lassau et al. (1999) studied 27 melanomas at 20 MHz and provided Doppler sonography analysis at 13 MHz. HFUS tumor thickness was in the range from 0.3 to 8.0 mm, whereas histological Breslow was in the range from 0.26 to 8.0 mm with a strong correlation ($r > 0.95$) [19]. Color Doppler results were compared with microvessel density (immunochemically with anti-factor VIII antibodies) and significantly correlated.

In 2002, Serrone et al. reported the differences in the correlation between 20 MHz HFUS and histology melanoma thickness measurements. One hundred ninety-three histologically confirmed melanomas were measured. A high correlation between HFUS and histomorphometry was found (r = 0.95), with an absolute difference of 0.32 ± 0.03 mm (mean ± SEM (standard error of the mean)) and a mean relative difference of 27.2% (95% confidence interval 23–31.4%). The highest correlation was found in melanoma > or = 1.51 mm thick and the lowest correlation in melanoma < or = 0.75 mm. 20 MHz HFUS was suggested useful for the surgical margin determining of > or = 0.76 mm thick lesions [20]. The 20 MHz HFUS accuracy in the preoperative staging of thin melanoma < or = 0.75 mm was suggested as limited.

In 2003, Pellacani and Seidenari measured 40 melanomas with 20 MHz HFUS and showed a good correlation (Pearson r = 0.89; $p < 0.001$)

between histologic and sonographic thickness. However, 15% of thin lesions (≤1 mm) were overestimated, and only 7% of thick lesions (>1 mm) were underestimated [21].

In 2008, Guitera et al. reported 52 melanomas' thickness at 75 MHz HFUS and Breslow histological index measurements, with a high correlation (Pearson's $r = 0.908$, $p < 0.001$). According to this study's results, the thin melanomas should be examined with a frequency higher than 20 MHz, and the advantage of 75 MHz sonography for this lesion was mentioned [22].

As the most frequent malignant skin tumor, BCC has been the subject of multiple clinical studies with HFUS in the last decades. One of the main goals was the accurate pretreatment BCC invasion depth and margins measurements and practical implementation of this diagnostic information in the treatment plan.

Desai et al. (2007) scanned 50 superficial and nodular BCCs at 20 MHz, delineated tumor margins before the surgical excision and histologic evaluation, and reported a good correlation with length and width ($r = 0.71$ and $r = 0.79$, respectively). In 45 cases from 50, the histological margins were clear, and in only 5 from 50 cases, the histological margins were positive [23].

In some studies, the HFUS BCC patterns were studied in detail, and this information was used for BCC types of noninvasive differentiation and proper treatment planning. Uhara et al. (2007) studied 30 BCCs at 15 and 30 MHz and described the hyperechoic spots in the tumor structure. The HFUS images were compared with the histological sections of the tumors after surgical excision. The hyperechoic spots were considered to correspond to calcification, horn cysts, or clusters of apoptotic cells in the centers of basal cell carcinoma nests and were proposed as differential characteristics between basal cell carcinoma and melanoma [24].

Bobadilla et al. (2008) studied 27 clinically BCC suspicious lesions on the face at 15 MHz [10]. In addition to the clinically visible lesions, two subclinical satellite neoplasms were found only with ultrasound. After HFUS evaluation, all 29 lesions were excised, and histology confirmed BCC diagnosis and excision with tumor-free borders in 100% of cases. The intraclass correlation coefficient (ICC) was used for the HFUS and histological BCC thickness measurement comparison. In 27 cases, ICC was excellent ≥0.9, and in 2 cases only, the tumor depths were overestimated.

Crisan et al. (2013) studied 18 BCCs at 20 MHz, followed by surgical excision and histological examination [1]. The clinical diagnosis was confirmed by histology in all cases, and complete removal of the tumor was also confirmed.

Hernández et al. (2014) summarized some critical HFUS applications, such as a differentiation possibility between BCC subtypes, tumor invasion depth measurement before treatment, and margin delineation with accurate advice for adequate surgical excision. They noted that rates of tumor-free margins in BCC excised after HFUS margin delimitation are as high as 95% (with the remark that the highest rates detected at nonaggressive BCC subtypes with easy HFUS access at low-risk sites) [25]. The trend for HFUS tumor size, especially length and width overestimation, was mentioned, which could be explained by ex vivo tissue shrinking during histological preparation. Some difficulties and limitations for HFUS BCC assessment are described, as difficult access to BCC high-risk sites (nose wings and folds, ears, and eyelids) and difficulties with accurate tumor margin determination for highly asymmetric lesions. Despite the mentioned limitations, HFUS was considered a useful and valuable tool for BCCs' and other tumors' assessment [25].

Further studies clarified the differential diagnostic signs of various BCC's clinical and morphological types. Wortsman et al. (2015) studied the presence of hyperechoic spots in the structure of 373 histologically confirmed BCCs and evaluated its relationship with tumors' histologic subtype and low (macronodular, superficial, adenoid cystic) or high (micronodular, sclerosing, infiltrating, morpheaform, and metatypical) recurrence risk. In HFUS examinations at 15 and 18 MHz [2], the hyperechoic spots were linked to the degree of malignancy. The amount of

hyperechoic spots in the high-recurrence-risk tumors (mean: 8; range: 4–81) was significantly higher than in low-recurrence-risk lesions (mean: 5.5; range: 3–25). Hence, a significant correlation was obtained between hyperechoic spots' presence and histologic high-risk BCC subtypes (p = 0.023). The largest hyperechoic spot number was found in micronodular BCCs, followed by sclerosing and morpheaform histologic BCC subtypes. The hyperechoic spots' number in the micronodular BCCs was significantly higher than that in the macronodular subtype. The count of ≥7 hyperechoic spots in BCC suggested a differential sign between high-recurrence-risk and low-recurrence-risk BCC subtypes, with a sensitivity of 79% and specificity of 53%. This study gives a new approach for clinically similar BCCs' differential diagnosis and high-risk histological subtypes' noninvasive preoperative prediction, vital for the choice of proper treatment options. The HFUS tumor margin delineation will help to provide incision with tumor-free margins.

Pasquali et al. (2016) proposed an original approach for HFUS postoperative BCC margin checkups. The 84 BCCs' invasion depth and margins were measured with HFUS at 22 MHz in vivo and ex vivo immediately after excision followed by histological examination [26]. In 81 cases, the HFUS and ex vivo and histology results matched (77 had negative and 4 had positive surgical margins). In 3 cases, ex vivo HFUS had one uncertain and two negative surgical margins, while positive surgical margins were detected with histology.

Hernández-Ibáñez et al. (2017) provided HFUS examination and punch biopsy of 156 different histologic BCC subtypes and compared results with excisional biopsy [27]. As a result, the HFUS overall diagnostic yield (73.7%: sensitivity 74.5%, specificity 73%) was close and comparable with punch biopsy (79.9%: sensitivity 76%, specificity 82%).

The different BCC subtypes have some specific HFUS patterns [1, 2, 13, 16, 23–25, 28–32].

The superficial BCC subtype is visualized as subepidermal flat, hypoechoic-heterogeneous zones, most often elongated with distinct (less often with irregular) contours without hypoechoic extensions into the underlying dermis.

The nodular BCCs featured hypoechoic zones of rounded or oval outlines and had the diffusely heterogeneous hypo-anechoic structure with distinct lateral and lower margins without projections to the surrounding dermis.

The morpheaform (sclerodermiform) subtype pattern featured hypoechoic-heterogeneous regions of irregular shape, infiltrating dermis. The increase in echogenicity around the tumor mass corresponds to the increase in edema and fibrosis often seen in these tumors.

The micronodular BCC subtype HFUS pattern is highly heterogeneous and consists of a hypoechoic/anechoic background with multiple hyperechoic spots. The shape is elongated with irregular lower boarders, and pseudopod-like infiltration of the underlying dermis.

Some HFUS BCC studies provided different high frequencies at 12, 15, 18, 20, 22, 30, 50, and 75 MHz [1, 28, 29, 31–34].

The minimal frequency for the skin examination regarding the European Federation of Societies for Ultrasound in Medicine and Biology (EFSUMB) recommendations is 15 MHz, and higher transducer frequencies may provide further information that may be relevant [35]. Color Doppler/power Doppler and pulsed spectral Doppler (in the case of vascular anomalies) are recommended to establish the inflammatory state of skin and appendages and the presence of skin lesion neovascularization.

In our practice, we use an 18 MHz array probe with color Doppler/power Doppler functions and 22, 33, 50, and 75 MHz single-crystal linear probes for the B-mode skin examination. This valuable combination can cover all skin lesions, and it is needed because frequency choice depends on the examination purpose and the tumoral depth.

15–18 MHz imaging with color Doppler/power Doppler is useful for detecting dermal and hypodermal lesions and borders imaging up to 35 mm depth, assessing tumor vascularization, inflammatory lesions, and vascular malformations.

A 20–33 MHz range is better for the dermis and upper subcutis imaging with a resolution of 80–48 microns on the depth up to 10–15 mm, depending on the transducer's focus.

The highest resolution of 31–21 μm is obtained at frequencies of 50–75 MHz. These are used to assess early or superficial lesions in the epidermis, dermis, and skin appendages. For example, for BCCs with a thickness of more than 10 mm, the frequency range of 14–18 MHz could be most helpful.

For tumors with a thickness of 4–10 mm, the 20–33 MHz range is commonly optimal. For the imaging of superficial and small nodular, sclerodermiform, and micronodular BCCs, with thickness of up to 3–4 mm, the frequency of 50 or 75 MHz could be used for a detailed study of the abnormalities in the epidermis and dermis. Even BCCs with a thickness of 50–100 μm could be visualized and measured at ultrahigh frequencies.

The combination of videodermoscopy in polarized and non-polarized light with HFUS examination is helpful as a kind of complex multimodal skin lesions' noninvasive diagnostics [18, 21, 36, 37]. Nowadays, most dermatologists are familiar with dermoscopy and use it as a routine diagnostic instrument. Therefore, the idea of combined dermoscopy and HFUS examinations could be practically helpful and positively accepted by clinicians, especially in early skin cancer diagnosis and treatment. The dermoscopic image helps the melanocytic and nonmelanocytic lesion differentiation and diagnosis, and HFUS detects tumor size, margins, and tissues involved in the pathologic process.

Clinical Cases

Case 1

Male patient, 63 years old, with a clinical diagnosis of nodular BCC on the nose tip, was examined with videodermoscopy and HFUS at 22 and 50 MHz in B-mode and 18 MHz in color Doppler mode. At videodermoscopy, the linear, irregular (serpentine), and glomerular vessels with multiple bends, blue ovoid nests, white blotches, and linear white areas are visualized. At B-scans, the hypoechoic and heterogeneous oval-shaped area measuring 6.1 mm × 3.9 mm and with posterior enhancement was visualized in the dermis and upper hypodermis. Some hyperechoic spots were detected at the tumor periphery. Color Doppler detected enhanced vascularity at the bottom part of the tumor body and underneath the tumor.

The lesion was excised with clear surgical margins. Histologic diagnosis (Mohs 45 method) confirmed a nodular BCC. In this case, the tumor was located in the dermis and upper layers of subcutaneous fat, so the frequency of 22 MHz was more suitable for the full BCC size and invasion depth measurements. The hyperechoic spots (arrows in Fig. 13.1a–c) correlated with the tumoral nests of atypical basaloid cells, which was described by Wortsman et al. in 2015. In this case, the hyperechoic spots were visualized at 18, 22, and 50 MHz, but at 50 MHz, the structure of the hyperechoic spots was more diffuse and visually matched with the basaloid macronodules in histological images (Fig. 13.1).

Clinical Case 2

Male patient, 58 years old, with a clinical diagnosis of nodular BCC on the nose tip, was examined with videodermoscopy and HFUS at 22 and 50 MHz in B-mode and 18 MHz in color Doppler mode. At videodermoscopy, the linear and irregular vessels, blue-gray ovoid nests, and peripheral leaflike pigmented structures are visualized.

At B-scans, the monomorphic hypo-anechoic oval-round-shaped area of 4.9 mm × 2.3 mm with weak posterior enhancement is visualized in the papillary and reticular dermis, not penetrating the subcutis. No vascularization was detected at the power Doppler examination. The tumor was excised with clear surgical margins.

Histologic diagnosis (Mohs method) demonstrated a nodular BCC. In this case, the tumor was located in the epidermis, and papillary and reticular dermis had a small size, so the frequency of 50 MHz was optimal for the accurate BCC margin delineation and invasion depth measurements (Fig. 13.2).

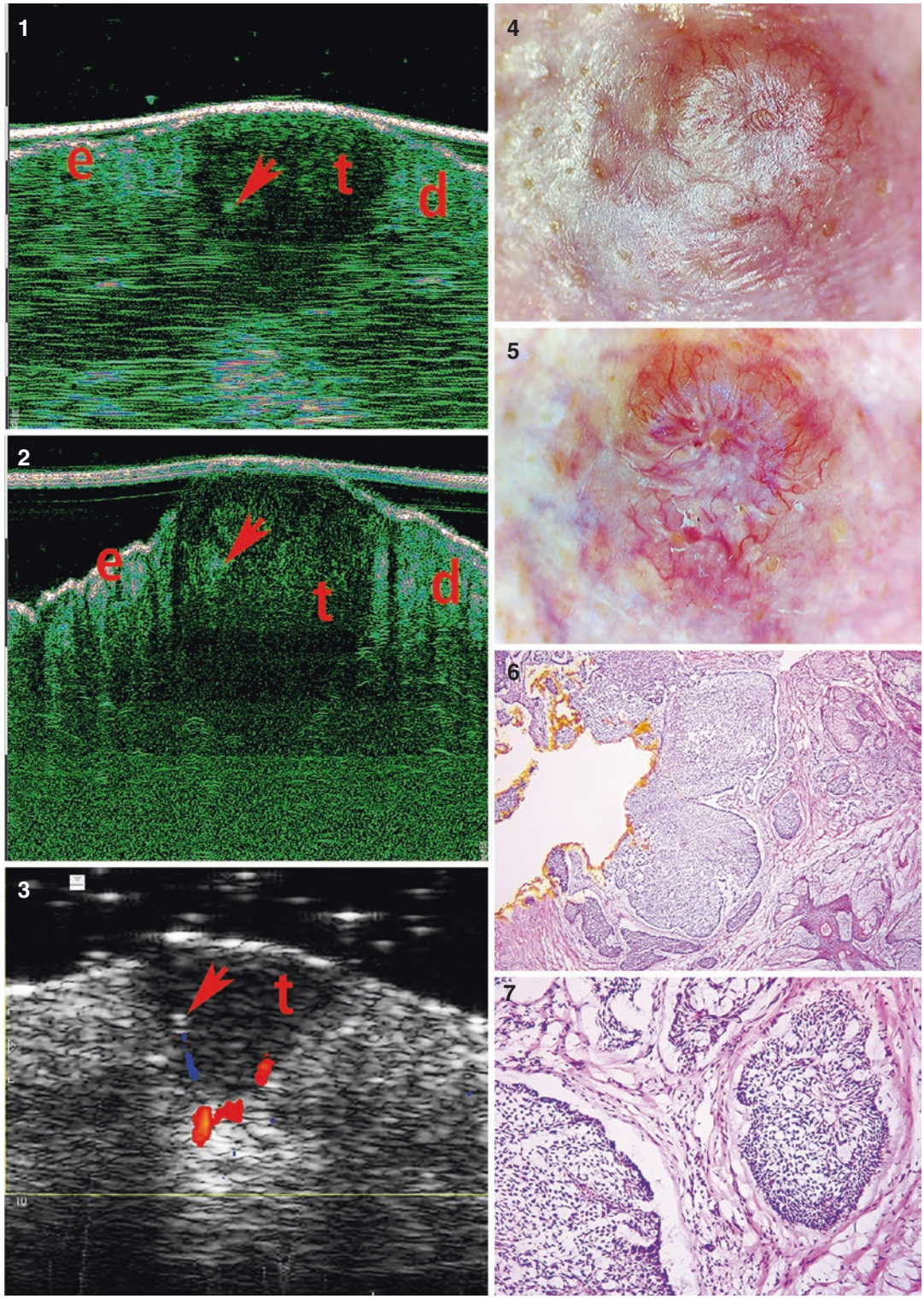

Fig. 13.1 Nodular BCC. B-mode 22 and 50 MHz scans, color Doppler, videodermoscopy, and histological images. (1) At 22 MHz scan, (2) at 50 MHz scan, (3) power Doppler, (4 and 5) videodermoscopy in non-polarized and polarized light, (6). histological image HE 50x, (7) histological image 200x. Abbreviations: *d* dermis, *e* epidermis, *t* tumor. Arrows, hyperechoic spots

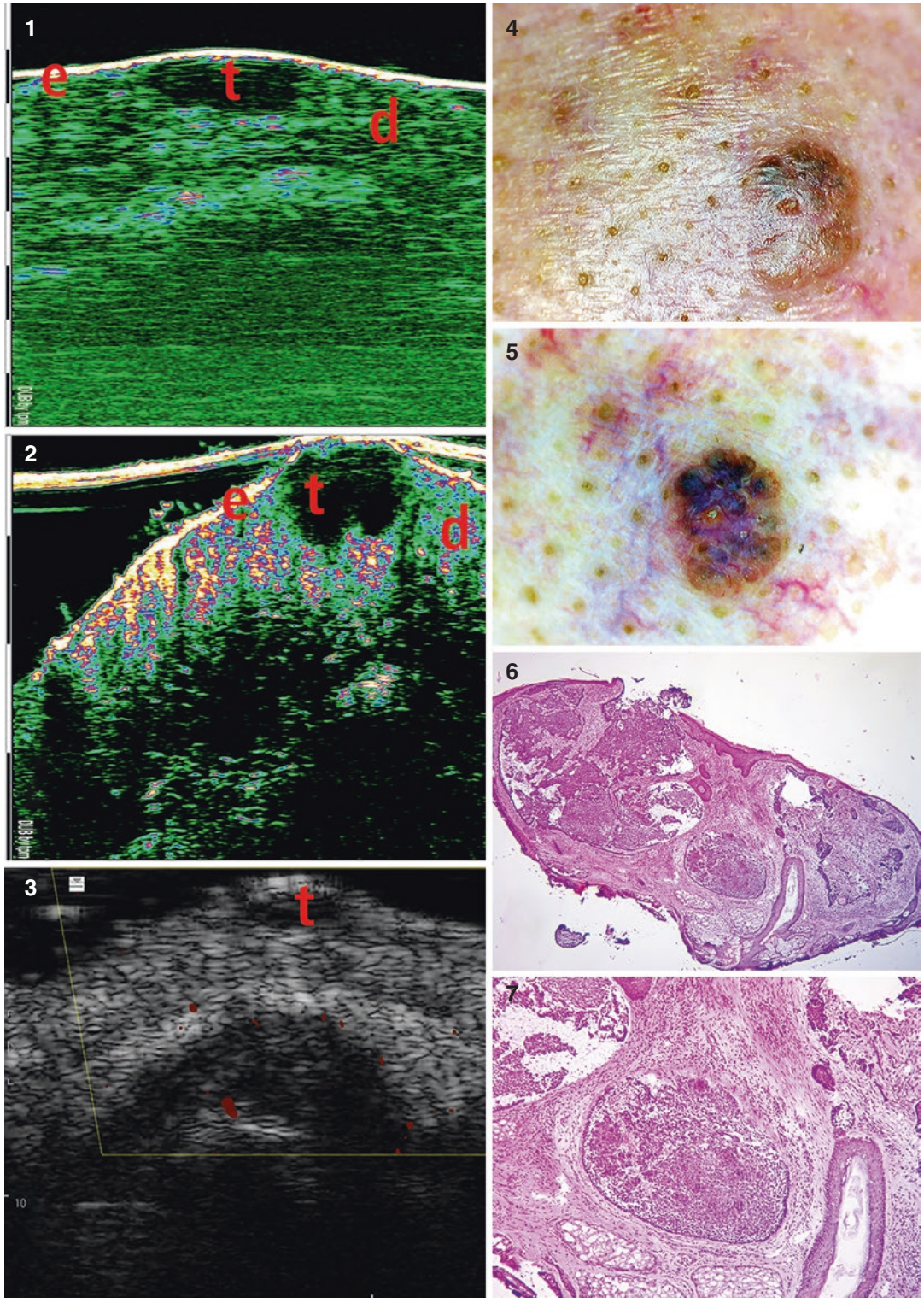

Fig. 13.2 Nodular BCC. (1) At 22 MHz, (2) at 50 MHz, (3) power Doppler, (4 and 5) videodermoscopy in non-polarized and polarized light, (6) histological image 50x, (7) histological image 200x. Abbreviations: *d* dermis, *e* epidermis, *t* tumor

Clinical Case 3

A female patient, 47 years old, with a clinical diagnosis of nodular BCC on the left temporal area, was examined with videodermoscopy and HFUS at 22 and 50 MHz in B-mode and 18 MHz in power Doppler mode. At videodermoscopy, the short, fine linear, and arborizing vessels, multiple blue globules, and translucent light-brown peripheral areas are visualized. At B-scans, the subepidermal hypoechoic-heterogeneous area of 8.8 mm × 0.4 mm was visualized in the papillary dermis with good demarcation from the underlying dermis. Multiple hypo-anechoic hair follicles presented at ROI. The 50 MHz images were compared with the contralateral area's control image to differentiate the hair follicles from the BCC invading pedicles. The tumor was excised with clear surgical margins. Histologic diagnosis (Mohs method) shows a superficial BCC. In this case, the tumor was located in the epidermis and papillary dermis and had an invasion depth of 0.4 mm. The frequency of 50 MHz was optimal for the accurate BCC margin delineation and invasion depth measurements (Fig. 13.3).

Case 4

Female, 37 years old, with a clinical diagnosis of superficial BCC on the forehead, was examined with videodermoscopy and HFUS at 22 and 50 MHz in B-mode and 18 MHz in color Doppler mode. At videodermoscopy multiple arborizing vessels, white homogenous areas, and short white streaks are visualized. At B-scans, the subepidermal nonuniform hypoechoic-heterogeneous area of 12.5 mm × 0.9 mm was visualized in the papillary and reticular dermis with an irregular lower margin. Multiple hypo-anechoic areas, looking like outgrowing sprouts, penetrated the tumor body in the underlying dermis. There was no vascularization increase at the color Doppler examination.

According to the dermoscopic and HFUS features, the tumor was supposed as the infiltrative micronodular or morpheaform subtype.

The tumor was excised with clear surgical margins. Histologic examination (Mohs method) showed an invasive micronodular BCC. In this case, the tumor was located in the epidermis, papillary, and particularly reticular dermis. The fine tumor structure with the irregular lower margin was clearly visualized with a 50 MHz probe. The small hypo-anechoic areas penetrating from the tumor body to the underlying dermis corresponded to the micronodular complexes (Fig. 13.4).

Case 5

Female, 49 years old, with clinical diagnosis nodular BCC located between left-eye inner canthus and nose wing, was examined with videodermoscopy and HFUS at 22 and 50 MHz in B-mode and 18 MHz in color Doppler mode. At videodermoscopy, multiple arborized vessels, white blotches, linear white structures, and white scales are visualized. At B-scans, the monomorphic hypo-anechoic oval-round-shaped area was 6.8 mm × 2.5 mm with posterior enhancement visualized in the papillary and reticular dermis, with the regular lower and lateral margins. Few hyperechoic spots were visualized at the central tumor part and the periphery. 0.5 mm lower under tumor bottom, the hypo-anechoic oval-shaped area of 3.7 mm × 1.2 mm was visualized at 5 o'clock direction. This area corresponded to the angular artery and vein projection. At color Doppler scans in this area, two blood vessels were visualized, and surgeons informed this feature. The tumor was excised with clear surgical margins. Histologic examination (Mohs method) showed a nodular BCC. The periarterial soft tissues were also excised, and the following histological examination did not find tumor structures in these tissues. In this case, the HFUS examination in B- and Doppler mode allowed the detection of very close nodular BCC and angular artery collocation. This diagnostic information was helpful for the safe tumor excision and decreased the artery injury risk (Fig. 13.5).

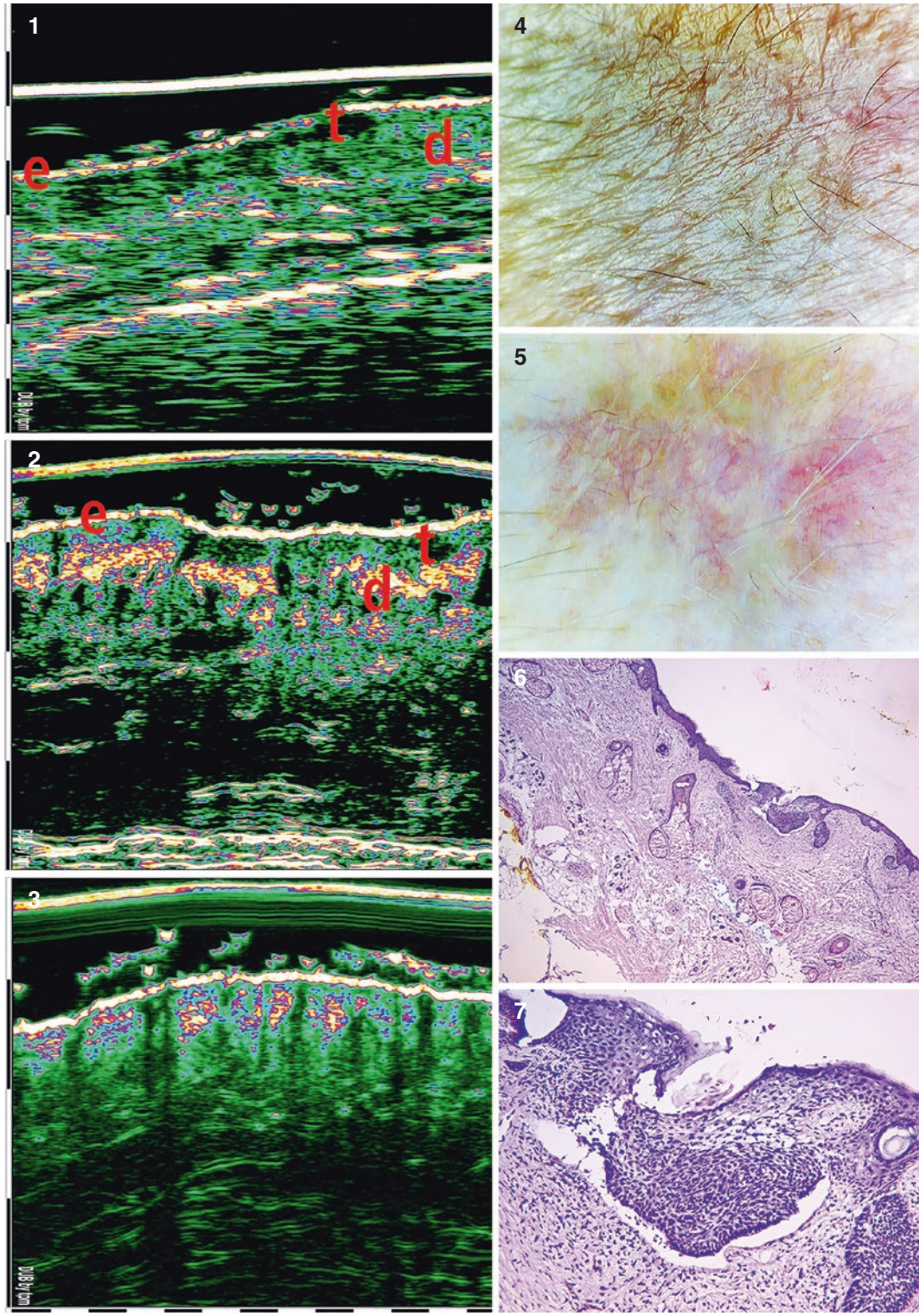

Fig. 13.3 Superficial BCC. B-mode 22 and 50 MHz scans, videodermoscopy, and histological images. (1) At 22 MHz, (2) at 50 MHz scan, (3) at 50 MHz, control intact skin image in the contralateral area, (4 and 5) videodermoscopy in non-polarized and polarized light, (6) histological image HE 50x, (7) histological image HE 200x. Abbreviations: *d* dermis, *e* epidermis, *t* tumor

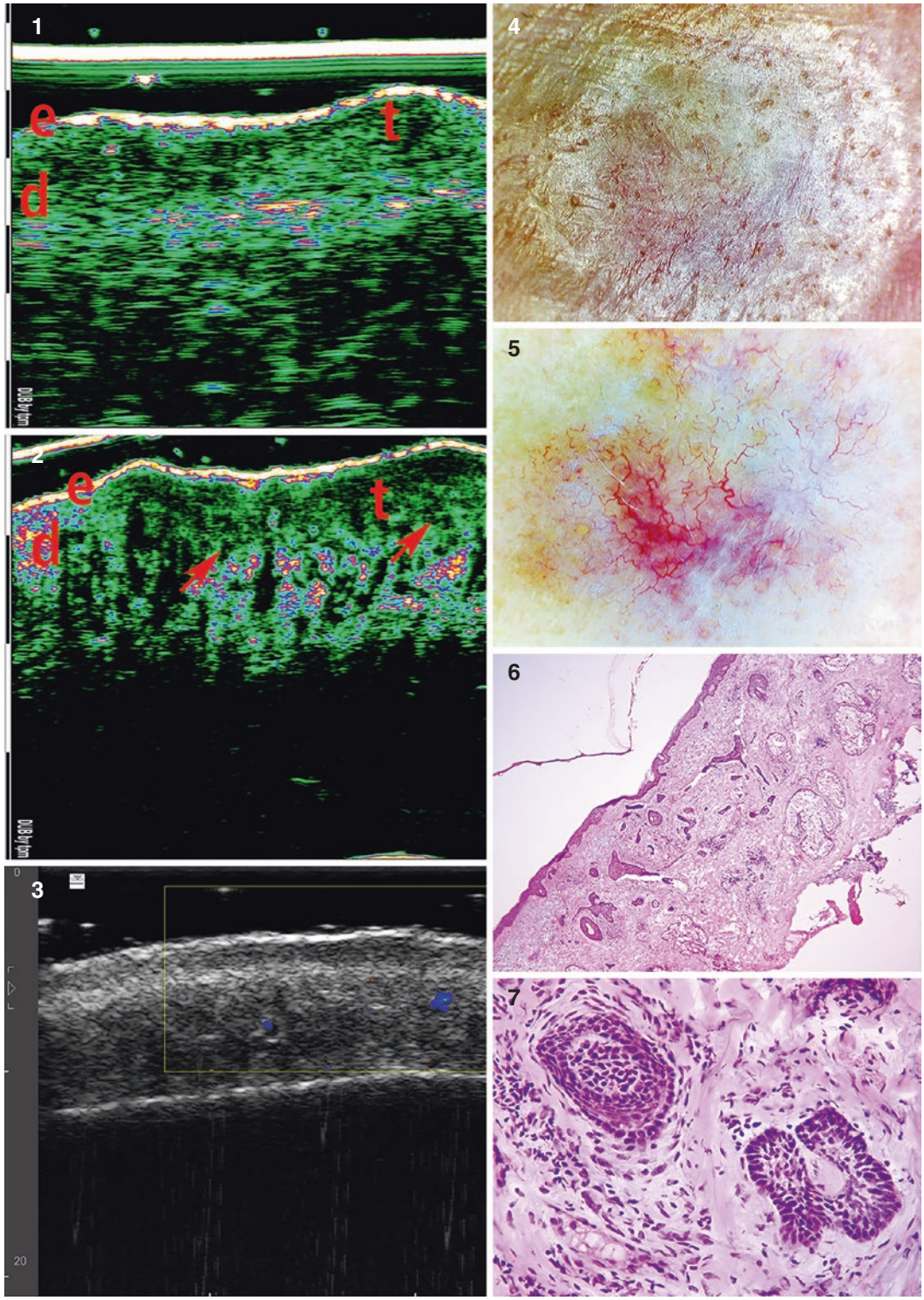

Fig. 13.4 Micronodular invasive BCC. B-mode 22 and 50 MHz scans, 18 MHz color Doppler scan, videodermoscopy, and histological images. (1) At 22 MHz, (2) at 50 MHz, (3) color Doppler scan at 18 MHz, (4 and 5) videodermoscopy in non-polarized and polarized light, (6) histological image HE 50x, (7) histological image HE 200x. The red arrow shows the invasive. Abbreviations: *d* dermis, *e* epidermis, *t* tumor

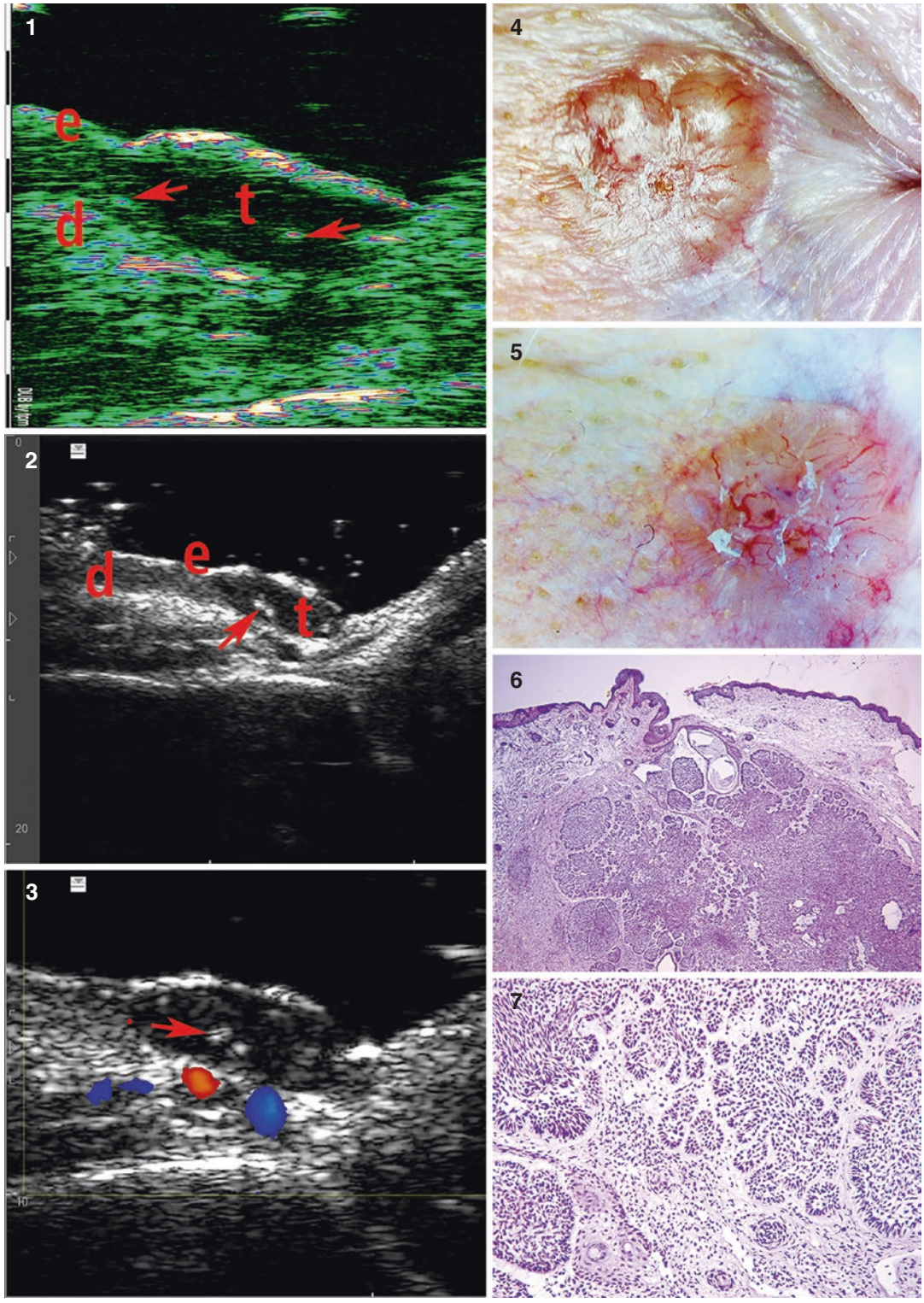

Fig. 13.5 Nodular BCC. B-mode 22 and 18 MHz scans, color Doppler, videodermoscopy, and histological images. (1) At 22 MHz scan, (2) at 18 MHz scan, (3) color Doppler at 18 MHz, (4 and 5) videodermoscopy in non-polarized and polarized light, (6) histological image HE 50x, (7) histological image HE 200x. The red arrows corresponded to hyperechoic spots. Abbreviations: *d* dermis, *e* epidermis, *t* tumor

Case 6

Female patient, 79 years old, with a clinical diagnosis of keratoacanthoma located on the left cheek, was examined with videodermoscopy and HFUS at 22 and 18 MHz in B-mode and 18 MHz in color Doppler mode. At videodermoscopy, the massive crust in the lesion center, multiple ringlike structures within the follicles, and linear-irregular and serpentine vessels are visualized. At 22 MHz B-scans, the crust located on the lesion top absorbed the ultrasound beam energy, and visualization of the underlying tissues was not possible. At 18 MHz scans, the hypoechoic-heterogeneous, oval-shaped 21.1 mm × 8.6 mm area with well-defined lateral and lower margins, with negative posterior shadow, was visualized in the dermis and subcutaneous fat. The tumor body was separated into some compartments with hyperechoic linear structures. At the color Doppler mode, weak vascularization at the tumor periphery was detected. The tumor was excised with clear surgical margins. Histologic examination (Mohs 45) showed a keratoacanthoma. In this case, HFUS examination at high frequencies of 22 and 50 MHz was not possible because of the large tumor size and the crust, reflecting the high-frequency ultrasound beam. The 18 MHz scanning and Doppler examination were helpful for the tumor size and margin measurement (Fig. 13.6).

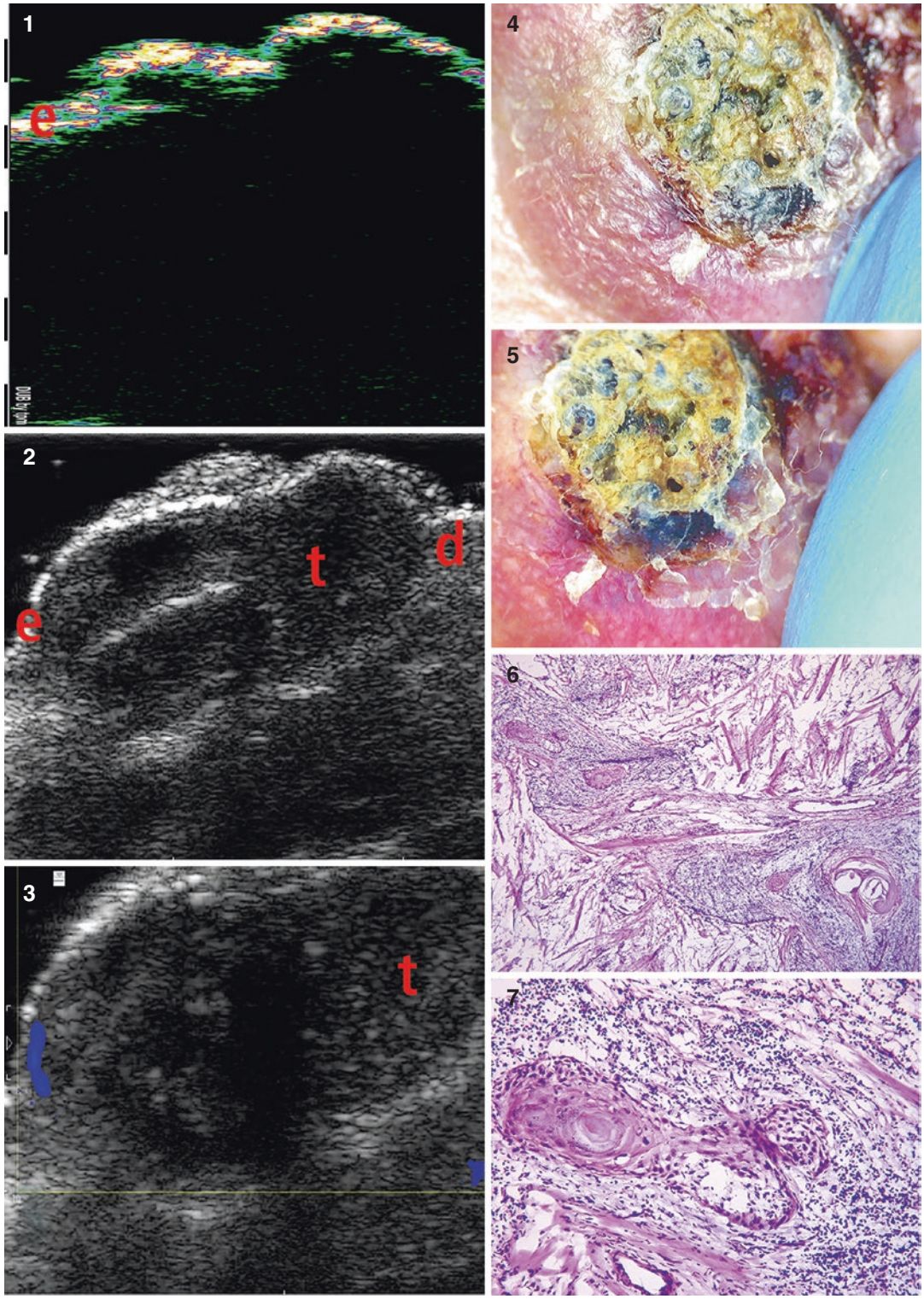

Fig. 13.6 Keratoacanthoma. B-mode 22 and 18 MHz scans, color Doppler, videodermoscopy, and histological images. (1) At 22 MHz scan, (2) at 18 MHz scan, (3) at color Doppler 18 MHz, (4 and 5) videodermoscopy in non-polarized and polarized light, (6) histological image HE 50x, (7) histological image HE 200x. Abbreviations: *d* dermis, *e* epidermis, *t* tumor

Conclusion

The high-frequency ultrasound is a valuable tool for nonmelanocytic skin cancer examination. HFUS was successfully used for the accurate tumor size and location measurement, invasion depth assessment, and tumor margin delineation. According to our practical experience, different frequencies should be used depending on the skin lesion size and depth. For small superficial lesions located in the epidermis and dermis (not deeper than 3–4 mm), the highest frequencies with the best resolution of 50–75 MHz are optimal. For the lesions with depths ≤10 mm, the frequencies of 20–33 MHz are helpful. If the lesion depth and size are ≥10 mm, the frequencies of 18–15 MHz, and sometimes lower, should be used for examination.

The multimodal skin tumor examination combining videodermoscopy (dermoscopy) and HFUS increases the diagnostic possibilities. Dermoscopic patterns described for the different skin cancer types have high sensitivity and specificity and are well known to most dermatologists and oncologists. The diagnostic HFUS value is essential for the preoperative/pretreatment tumor assessment for the proper treatment tactic choice. Moreover, the HFUS patterns provide information about internal tumor morphology and correlate with histology, and in many cases allow differentiation between melanoma, BCC, and SCC. Experienced specialists could recognize even different histological BCC subtypes. We hope that the HFUS skin diagnostics will soon become the standard tool in dermatologic and oncologic clinics.

References

1. Crisan M, Crisan D, Sannino G, Lupsor M, Badea R, Amzica F. Ultrasonographic staging of cutaneous malignant tumors: an ultrasonographic depth index. Arch Dermatol Res. 2013;305(4):305–13.
2. Wortsman X, Vergara P, Castro A, Saavedra D, Bobadilla F, Sazunic I, Zemelman V, Wortsman J. Ultrasound as predictor of histologic subtypes linked to recurrence in basal cell carcinoma of the skin. J Eur Acad Dermatol Venereol. 2015;29(4):702–7.
3. Davydov MI, Axel EM. Statistics of malignant neoplasms in 2014. Eurasian Oncol J. 2016;4(4):692–879. (In Russ.)
4. Shlyakhtunov EA, Hydranovich AV, Lud NG. Skin cancer: the current state of the problem. Bull VSMU. 2014;13(3):20–8. (In Russ.)
5. Kohlmeyer J, Steimle-Grauer SA, Hein R. Cutaneous sarcomas. J Dtsch Dermatol Ges. 2017;15(6):630–48.
6. Que SKT, Zwald FO, Schmults CD. Cutaneous squamous cell carcinoma: incidence, risk factors, diagnosis, and staging. J Am Acad Dermatol. 2018;78(2):237–47.
7. Chebotarev VV, Khismatullina ZR, Zakirova YA. Some aspects of the epidemiology and diagnostics of malignant skin neoplasms. Creat Surg Oncol. 2020;10(1):65–73. (In Russ.)
8. Dinnes J, Deeks JJ, Chuchu N, Ferrante di Ruffano L, Matin RN, Thomson DR, Wong KY, Aldridge RB, Abbott R, Fawzy M, Bayliss SE, Grainge MJ, Takwoingi Y, Davenport C, Godfrey K, Walter FM, Williams HC. Cochrane skin cancer diagnostic test accuracy group. Dermoscopy, with and without visual inspection, for diagnosing melanoma in adults. Cochrane Database Syst Rev. 2018;12(12):CD011902.
9. Wortsman X, Jemec GBE. High resolution ultrasound applications in dermatology. Rev Chilena Dermatol. 2006;22:37–45.
10. Bobadilla F, Wortsman X, Mu˜noz C, Segovia L, Espinoza M, Jemec GBE. Pre-surgical high resolution ultrasound of facial basal cell carcinoma: correlation with histology. Cancer Imaging. 2008;8:163–72.
11. Schwaighofer B, Pohl-Markl H, Frühwald F, Stiglbauer R, Kokoschka EM. Der diagnostische Stellenwert des Ultraschalls beim malignen Melanom [Diagnostic value of ultrasound in malignant melanoma]. Rofo. 1987;146(4):409–11. German.
12. Hoffmann K, el Gammal S, Matthes U, Altmeyer P. Digitale 20 MHz-Sonographie der Haut in der präoperativen Diagnostik [Digital 20 MHz sonography of the skin in preoperative diagnosis]. Z Hautkr. 1989;64(10):851–2–5–8. German.
13. Hoffmann K, Stücker M, el-Gammal S, Altmeyer P. Digitale 20-MHz-sonographie des basalioms im B-scan [Digital 20 MHz sonography of basalioma in the B-scan]. Hautarzt. 1990;41(6):333–9. German.
14. Gassenmaier G, Kiesewetter F, Schell H, Zinner M. Wertigkeit der hochauflösenden Sonographie für die Bestimmung des vertikalen Tumordurchmessers beim malignen Melanom der Haut [Value of high resolution ultrasound in determination of vertical tumor thickness in malignant melanoma of the skin]. Hautarzt. 1990;41(7):360–4. German.
15. Bahmer FA, Schild R. Die vertikale Tumordicke als Schätzer des tatsächlichen Tumorvolumens [Vertical tumor thickness as an estimate of actual tumor volume]. Z Hautkr. 1990;65(10):901–4. German.
16. Harland CC, Bamber JC, Gusterson BA, Mortimer PS. High frequency, high resolution B-scan ultrasound in the assessment of skin tumours. Br J Dermatol. 1993;128(5):525–32.

17. Gupta AK, Turnbull DH, Foster FS, Harasiewicz KA, Shum DT, Prussick R, Watteel GN, Hurst LN, Sauder DN. High frequency 40-MHz ultrasound. A possible noninvasive method for the assessment of the boundary of basal cell carcinomas. Dermatol Surg. 1996;22(2):131–6.
18. Krähn G, Gottlöber P, Sander C, Peter RU. Dermatoscopy and high frequency sonography: two useful non-invasive methods to increase preoperative diagnostic accuracy in pigmented skin lesions. Pigment Cell Res. 1998;11(3):151–4.
19. Lassau N, Mercier S, Koscielny S, Avril MF, Margulis A, Mamelle G, Duvillard P, Leclère J. Prognostic value of high-frequency sonography and color Doppler sonography for the preoperative assessment of melanomas. AJR Am J Roentgenol. 1999;172(2):457–61.
20. Serrone L, Solivetti FM, Thorel MF, Eibenschutz L, Donati P, Catricalà C. High frequency ultrasound in the preoperative staging of primary melanoma: a statistical analysis. Melanoma Res. 2002;12(3):287–90.
21. Pellacani G, Seidenari S. Preoperative melanoma thickness determination by 20-MHz sonography and digital videomicroscopy in combination. Arch Dermatol. 2003;139(3):293–8.
22. Guitera P, Li LX, Crotty K, Fitzgerald P, Mellenbergh R, Pellacani G, Menzies SW. Melanoma histological Breslow thickness predicted by 75-MHz ultrasonography. Br J Dermatol. 2008;159(2):364–9.
23. Desai TD, Desai AD, Horowitz DC, Kartono F, Wahl T. The use of high-frequency ultrasound in the evaluation of superficial and nodular basal cell carcinomas. Dermatol Surg. 2007;33(10):1220–7.
24. Uhara H, Hayashi K, Koga H, Saida T. Multiple hypersonographic spots in basal cell carcinoma. Dermatol Surg. 2007;33:1215–9.
25. Hernández C, del Boz J, de Troya M. Can high-frequency skin ultrasound be used for the diagnosis and management of Basal cell carcinoma? Actas Dermosifiliogr. 2014;105(2):107–11. English, Spanish.
26. Pasquali P, Freites-Martinez A, Fortuño-Mar A. Ex vivo high-frequency ultrasound: a novel proposal for management of surgical margins in patients with non-melanoma skin cancer. J Am Acad Dermatol. 2016;74(6):1278–80.
27. Hernández-Ibáñez C, Blazquez-Sánchez N, Aguilar-Bernier M, Fúnez-Liébana R, Rivas-Ruiz F, de Troya-Martín M. Usefulness of high-frequency ultrasound in the classification of histologic subtypes of primary basal cell carcinoma. Actas Dermosifiliogr. 2017;108(1):42–51.
28. Khlebnikova AN, Molochkov VA, Selezneva EV, Belova LA, Bezugly A, Molochkov AV. Ultrasonographic features of superficial and nodular basal cell carcinoma. Med Ultrason. 2018;20(4):475–9.
29. Khlebnikova A, Molochkov V, Selezneva E, Belova L, Bezugly A, Sedova T, Molochkov A. Basal cell carcinoma invasion depth determined with 30 and 75 MHz high-frequency ultrasound and histopathology - a comparative study. Med Ultrason. 2020;22(1):31–6.
30. Catalano O, Roldán FA, Varelli C, Bard R, Corvino A, Wortsman X. Skin cancer: findings and role of high-resolution ultrasound. J Ultrasound. 2019;22(4):423–31.
31. Wang SQ, Liu J, Zhu QL, Zhao CY, Qu T, Li F, Wortsman X, Jin HZ. High-frequency ultrasound features of basal cell carcinoma and its association with histological recurrence risk. Chin Med J. 2019;132(17):2021–6.
32. Qin J, Wang J, Zhu Q, Liu J, Gao Y, Wang Y, Jin H. Usefulness of high-frequency ultrasound in differentiating basal cell carcinoma from common benign pigmented skin tumors. Skin Res Technol. 2021;27(5):766–73.
33. Bezugly A. High frequency ultrasound study of skin tumors in dermatological and aesthetic practice. Med Ultrason. 2015;17(4):541–4.
34. Kim HJ, Lee SJ, Lee JH, Shin SH, Xu H, Yang I, Kim JH, Kim SH, Suh IS. Usefulness of ultrasonography in determining the surgical excision margin in non-melanocytic skin cancer: a comparative analysis of preoperative ultrasonography and postoperative histopathology. Medicine (Baltimore). 2020;99(51):e23789.
35. Alfageme F, Wortsman X, Catalano O, Roustan G, Crisan M, Crisan D, Gaitini DE, Cerezo E, Badea R. European Federation of Societies for ultrasound in medicine and biology (EFSUMB) position statement on dermatologic ultrasound. Ultraschall Med. 2021;42(1):39–47.
36. Barcaui Ede O, Carvalho AC, Valiante PM, Barcaui CB. High-frequency ultrasound associated with dermoscopy in pre-operative evaluation of basal cell carcinoma. An Bras Dermatol. 2014;89(5):828–31.
37. Hayashi K, Uhara H, Okuyama R. Detection of the tumor margin of basal-cell carcinoma using dermoscopy and high-frequency ultrasound with narrow pieces of surgical tape as skin markers. Dermatol Surg. 2014;40(6):704–6.